THERMAL GRADIENT IN THE LUNAR SOUTH POLAR REGION ESTIMATED FROM INFRARED AND MICROWAVE OBSERVATIONS. J. Feng[1], M. A. Siegler[1], [1]Planetary Science Institute (1700 East Fort Lowell, Suite 106 Tucson, AZ 85719-2395, jfeng@psi.edu).

Introduction: Lunar polar region is an ideal place to study the thermophysical properties of lunar regolith at low temperatures (<100K). The long-term stability of water ice in the permanent shadowed region (PSR) depends on regolith's subsurface temperature and thermal properties. Previous studies [1] show the thermal inertia of lunar regolith fines are remarkably uniform. However, Far-ultraviolet reflectance properties indicates that the surface regolith in PSRs may have much larger porosities than non-PSR regions [2]. Also, extremely low temperatures in PSRs (as low as 20 K) are observed by Lunar Reconnaissance Orbiter (LRO) Diviner Lunar Radiometer Experiment [3], revealing apparently lower thermal inertia than explainable by existing theory.

Woods-Robinson et al. [4] derive a semiempirical model of specific heat and thermal conductivity of lunar regolith in a temperature range of 20-400 K from measurements of lunar simulants. Their results show the thermal conductivity is as much as an order of magnitude lower than expected from current models. To better understand the thermal behavior of regolith in lunar polar region, we use the data from Diviner and Chang'e-2 (CE-2) microwave radiometer (MRM) to estimate subsurface density and thermal gradients.

Data set: The CE-2 MRM measured the brightness temperature (T_B) of the moon in 2010-2011 with a space resolution of approximately 25 km at 3 GHz and 17.5 km at 7.8, 19.35, 37 GHz. The overlapping ratio between adjacent observations is very high along the track (~ 80%). Also, near the pole the MRM measurements is much denser than low latitude. This gives a feasibility to make higher resolution maps in polar regions. South-polar maps of mean T_B at 3 GHz with a resolution of 5 km is made. The 3-GHz T_B is adjusted by adding 10 K and data at terminator orbit are excluded because of contamination on calibration horn [5].

Diviner is a nine-channel visible and infrared instrument which has been observing the Moon for over 10 years. It provides an excellent constraints of surface temperature variation in polar region. Recently [3] compiled these data into polar maps of the summer and winter seasonal temperatures at a resolution of 240 m. We average the yearly temperature and resample the map into 5 km/pixel. To simulate the convolution effect of MRM data, the map is smoothed by a 2-D gaussian filter with a window of 25 km × 25 km.

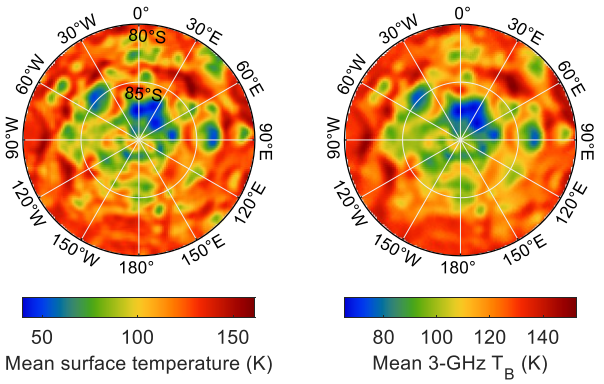

Fig. 1. (a) Resampled and filtered $\bar{T}_s$ with a resolution of 5 km. (b) Mean 3-GHz T_B in the lunar south polar region binned with a resolution of 5 km.

Approach and Methods: Due to low temperature at high latitude area, the radiative component in thermal conductivity becomes very small, which results in an almost linear mean-temperature profile within the regolith. Therefore, the mean temperature profile of a specific location could be expressed by

$$\bar{T}_{(z)} = \bar{T}_s + gz \quad (1)$$

where $\bar{T}_{(x)}$ is the mean temperature at depth of x. $\bar{T}_s$ is the mean surface temperature and b is the average thermal gradient. According to the 1-D incoherent radiative transfer model [7], the T_B of a semi-infinite scatter-free homogeneous medium under nadir observation is given by

$$T_B = (1 - \Gamma) \int_0^\infty \kappa_\alpha T_{(z)}\, e^{-\kappa_\alpha z} dz \quad (2)$$

where Γ is the reflectivity on the surface boundary and κ_α is the power absorption coefficient which is a function of frequency, dielectric permittivity, and loss tangent. The discrete form of formula (2) is $T_B = \sum_{i=1}^{n} W_i T_i$. Thus, the yearly average $\bar{T}_B$ can be written as

$$\bar{T}_B = \sum \bar{T}_i W_i = \sum (\bar{T}_s + \bar{g} z_i) W_i \quad (3)$$

where z_i and W_i is the depth and weighting function of i-th layer [5]. Formula (8) can be transformed to:

$$\bar{g} = \frac{(\bar{T}_B - \bar{T}_s \sum W_i)}{\sum z_i W_i} \quad (4)$$

Formula (4) shows that once W_i and z_i is known, the mean temperature gradient $\bar{g}$ could be calculated from $\bar{T}_s$ and $\bar{T}_B$. Here we first assume that in the polar region the regolith has the same density and layering structure as at equator. Then we can use a standard weighting function to compute $\bar{g}$ anywhere in the polar regions. The profile of W_i at a certain frequency could be determined only by a density profile and the thickness of each layer [5, 6]. Based on the generated 3-GHz $\bar{T}_B$ and

$\bar{T}_s$ maps in Figure 1 and the 3-GHz weighting function, the thermal gradient map of the lunar south polar region is derived from Equation (4) as shown in Figure 2.

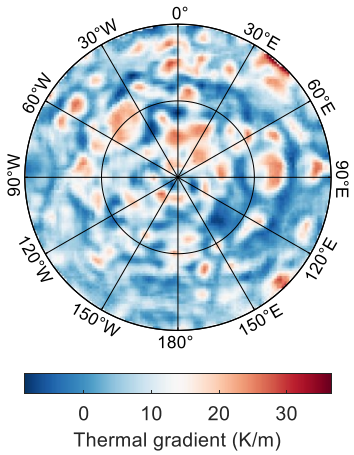

Fig. 2. Relative thermal gradient in the lunar south polar region. This is calculated based on an assumption that the regolith everywhere has the same density structure.

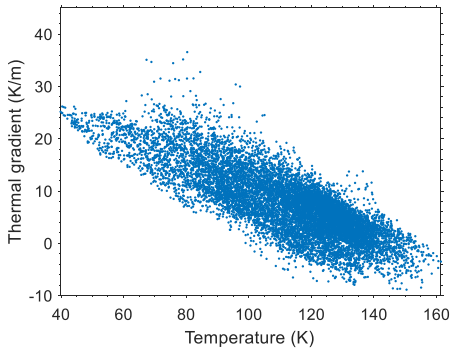

Fig. 3. Mean surface temperature vs thermal gradient in lunar south polar region

Figure 2 and thermal gradient vs mean surface temperature (Figure 3) suggest that some largest thermal gradient happen in PSRs (except some anomalies in the edge of map). What's more, the thermal gradient has a linear relationship with mean surface temperature, which implies the thermal conductivity has a temperature dependence.

Figure 4 shows an example of how PSR model predictions based on the thermal conductivity proposed by Woods-Robinson [4] match well with Diviner and Chang'E-2 data, lending confidence to this model approach. The H-parameter is 0.40 m in the Shoemaker.

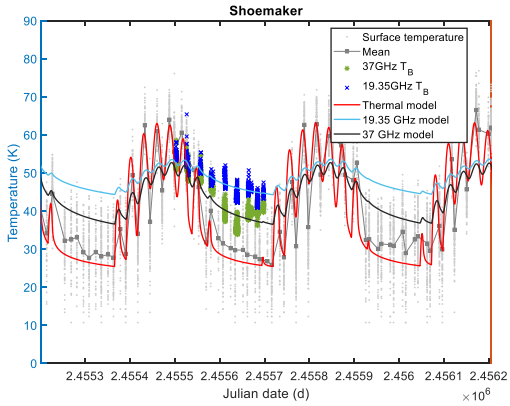

Fig. 4. Surface temperature and T_B at 19.35 and 37 GHz in Shoemaker crater and models.

Conclusion: We use the mean surface temperature measured by Diviner and brightness temperature at 3 GHz from CE-2 MRM to calculate the thermal gradient in lunar south polar region. Our results show that the thermal gradient decrease with temperature. PSRs have the largest thermal gradient. We believe this is due to low density of regolith and substantial temperature dependence of thermal conductivity at low temperature.

References:

[1] Hayne, P. et al. (2017) *JGR*,122, 2371-2400. [2] Gladstone, R. et al. (2012) *JGR*, 117, E00H04. [3] Williams, J. et al. (2012) *JGR*, 124, 2505-2521. [4] Woods-Robinson, R. et al. (2019) *JGR*, 124, 1989-2011. [5] Feng, J. et al. (2020) *JGR*, 125, e2019JE006130. [6] Siegler, M. et al. 2020, 125: e2020JE006405. [7] Ulaby, F. et al. (1981), Addison-Wesley Pub.